Appl Microbiol Biotechnol (2015) 99:10047–10056
DOI 10.1007/s00253-015-6889-2

Improvement in the thermostability of a type A feruloyl esterase, AuFaeA, from *Aspergillus usamii* by iterative saturation mutagenesis

Xin Yin[1] · Jian-Fang Li[2] · Chun-Juan Wang[2] · Die Hu[1] · Qin Wu[1] · Ying Gu[3] · Min-Chen Wu[3]

Received: 5 May 2015 / Revised: 5 July 2015 / Accepted: 28 July 2015 / Published online: 13 August 2015

Abstract Feruloyl or ferulic acid esterase (Fae, EC 3.1.1.73) catalyzes the hydrolysis of ester bonds between polysaccharides and phenolic acid compounds in xylan side chain. In this study, the thermostability of a type A feruloyl esterase (AuFaeA) from *Aspergillus usamii* was increased by iterative saturation mutagenesis (ISM). Two amino acids, Ser33 and Asn92, were selected for saturation mutagenesis according to the B-factors analyzed by B-FITTER software and ΔΔG values predicted by PoPMuSiC algorithm. After screening the saturation mutagenesis libraries constructed in *Pichia pastoris*, 15 promising variants were obtained. The best variant S33E/N92-4 (S33E/N92R) produced a T_m value of 44.5 °C, the half-lives ($t_{1/2}$) of 35 and 198 min at 55 and 50 °C, respectively, corresponding to a 4.7 °C, 2.33- and 3.96-fold improvement compared to the wild type. Additionally, the best S33 variant S33-6 (S33E) was thermostable at 50 °C with a $t_{1/2}$ of 82 min, which was 32 min longer than that of the wild type. All the screened S33E/N92 variants were more thermostable than the best S33 variant S33-6 (S33E). This work would contribute to the further studies on higher thermostability modification of type A feruloyl esterases, especially those from fungi. The thermostable feruloyl esterase variants were expected to be potential candidates for industrial application in prompting the enzymic degradation of plant biomass materials at elevated temperatures.

Keywords Feruloyl esterase · *Aspergillus usamii* · Thermostability · Iterative saturation mutagenesis

Introduction

Xylan is a predominant form of hemicellulose, in which arabinose, glucuronic acid, feruloyl, coumaroyl, and/or acetyl ester groups existed as side chains link with the xylose residues (Rakotoarivonina et al. 2011). Due to the heterogeneity and complexity of xylans, their complete degradation requires an enzyme system of several hydrolytic enzymes, such as β-1,4 endoxylanases, arabinofuranosidases, glucuronidases, β-1,4 xylosidases, and carbohydrate esterases (Shallom and Shoham 2003). Among them, feruloyl esterase (EC 3.1.1.73), belonging to a subfamily of the carbohydrate esterase family, plays a crucial role in xylan degradation, since it catalyzes the hydrolysis of ester bonds between polysaccharides and phenolic acid compounds in the xylan side chain. It can be applied in biotechnological processes, for example, in the deconstruction of hemicellulose for biofuel production, pharmaceutical, pulp and paper, and animal feed and food industries (Faulds 2010). On the basis of the substrate preference and primary structure homology, feruloyl esterases have been classified into four types: types A, B, C, and D (Crepin et al. 2004). Types A and B feruloyl esterases are the best studied. Hitherto, crystallographic structure of a type A feruloyl esterase from *Aspergillus niger* has been analyzed. Its structure is based on an α/β hydrolase fold and consists

Xin Yin and Jian-Fang Li, the two first authors, contributed equally to this work.

✉ Min-Chen Wu
biowmc@126.com

[1] Key Laboratory of Carbohydrate Chemistry and Biotechnology, Ministry of Education, School of Biotechnology, Jiangnan University, 1800 Lihu Road, Wuxi 214122, China

[2] State Key Laboratory of Food Science and Technology, School of Food Science and Technology, Jiangnan University, 1800 Lihu Road, Wuxi 214122, China

[3] Wuxi Medical School, Jiangnan University, 1800 Lihu Road, Wuxi 214122, China

of a major nine-stranded mixed β-sheet, two minor two-stranded β-sheet arrangements, and seven helixes. Moreover, there are three disulfide bridges located in this feruloyl esterase simulating three legs of a tripod (Hermoso et al. 2004).

Thermophilic enzymes are more favorable than mesophilic counterparts in many bioprocesses, such as in pulp bleaching and feedstuff preparation, since high temperatures are commonly encountered, which can enhance the mass transfer rate, reduce the substrate viscosity and the risk of contamination (Badieyan et al. 2012; Turner et al. 2007). A handful of thermophilic enzymes have been obtained from thermophiles, but their other enzymatic properties, such as kinetic parameters and specific activities, are poor, making them unable to be applied effectively. Particularly, thermostable feruloyl esterase remains scarce. Few reported thermostable feruloyl esterases were of thermophilic source. For example, a type A TtFAE from *Thermoanaerobacter tengcongensis* was highly thermostable, and its half-lives ($t_{1/2}$) were calculated to be >600 min at 75 °C and 50 min at 80 °C (Abokitse et al. 2010). Another type B Tx-Est1 from *Thermobacillus xylanilyticus* was identified with the temperature optimum of 65 °C (Rakotoarivonina et al. 2011). In general, those thermostable feruloyl esterases were not only in low activities but also in low identities with the mesophilic ones from fungi for their primary structures. A majority of feruloyl esterases with excellent properties from thermolabile organisms were mesophilic (Zhang et al. 2013; Zhang and Wu 2011). It is necessary to improve the thermostability of those mesophilic enzymes with superior properties. Therefore, protein engineering of mesophilic feruloyl esterases is an important strategy to obtain thermostable ones.

Many methods have been applied to increase the protein thermostability, such as error-prone PCR technique, DNA shuffling, site-directed mutagenesis, and regional substitution (Chen et al. 2014; Stephens et al. 2014; Zhang et al. 2014; Zheng et al. 2014). In recent years, iterative saturation mutagenesis (ISM) has been developed as an efficient approach for protein engineering. It has been successfully applied not only to evolve many enzymes with enantioselectivity, regioselectivity, and expanded substrate scope but also to modify the protein thermostability (Li and Cirino 2014). Using the ISM method, the T_{50}^{15} values (temperature at which a heat treatment for 15 min results in 50 % activity loss) of mutants IV, VII, VIII, and IX of a lipase from *Bacillus subtilis* (BSL) were increased by 4, 8, 10, and 13 °C than that of the wild type, respectively. Particularly, the T_{50}^{60} value of XI was increased from 48 to 93 °C (Reetz et al. 2010). The selection of amino acid positions for ISM is extremely important, which can be based on the B-factor values (an atomic displacement parameter), ΔΔG values (the protein changes in folding free energy), or other parameters. The amino acids in a protein with the highest B-factors were corresponded to the most pronounced degrees of thermal motion and thus flexible (Reetz et al. 2006). The ΔΔG values of proteins were predicted by a web server PoPMuSiC algorithm using a linear combination of statistical potentials whose coefficients depend on the solvent accessibility of the mutated residue, which showed the thermodynamic stability changes caused by single-site mutations in proteins (Dehouck et al. 2011). A RGI lyase mutant E434L was emerged according to the B-factor and ΔΔG values, which produced a half-life of 31 min at 60 °C, a 1.6-fold improvement of the thermostability compared to its wild type (Silva et al. 2013). In our previous work, a mesophilic type A feruloyl esterase (AuFaeA) (GenBank accession no AHB63528) from *Aspergillus usamii* E001 was expressed in *Pichia pastoris* (Gong et al. 2013). Now, based on the B-factors and ΔΔG values of a type A feruloyl esterase from *A. niger* (AnFaeA, PDB code 1UWC), which has 98 % identity with AuFaeA for their primary structures, ISM was implemented to AuFaeA for its thermostability enhancement. This work would contribute to the further studies on higher thermostability modification of type A feruloyl esterases, especially those from fungi.

Materials and methods

Strains, plasmids, and culture media

Escherichia coli JM109 and plasmid pPIC9K (Invitrogen, San Diego, CA, USA) were used for constructing the recombinant expression plasmids. The plasmid pUCm-T (Sangon, Shanghai, China) was used for gene cloning and DNA sequencing. The gene *AufaeA* (GenBank accession no KF805148) has been inserted into the pPIC9K, resulting a recombinant expression plasmid pPIC9K-*AufaeA*, which was constructed and preserved in our laboratory (Gong et al. 2013). *E. coli* JM109 was cultured in the LB medium (10 g/l tryptone, 5 g/l yeast extract, and 10 g/l NaCl, pH 7.2). *P. pastoris* GS115 and its transformants were cultured and methanol-induced in the YPD, MD, BMGY, and BMMY media, which were prepared as described in the manual of Multi-Copy *Pichia* Expression Kit (Invitrogen, USA).

Analysis of primary and three-dimensional structures

Homology sequence search at the NCBI website (http://www.ncbi.nlm.nih.gov/) was performed using the BLAST server, and homology alignment of protein primary structures was analyzed using the ClustalW2 program (http://www.ebi.ac.uk/Tools/msa/clustalw2/). The three-dimensional (3D) structures of *A. usamii* AuFaeA and its variants were homologically modeled and optimized using the MODELLER 9.9 program (http://salilab.org/modeller/) with the crystal structure of AnFaeA (PDB code 1UWC) as a template. The B-factor

values of the whole amino acid residues of AnFaeA (1UWC) were analyzed by B-FITTER software (http://www.mpi-muelheim.mpg.de/reetz.html). The ΔΔG values of AnFaeA were predicted by PoPMuSiC algorithm (http://dezyme.com/). The 3D structure was visualized using a PyMOL software (http://pymol.org). The intramolecular interactions in protein were analyzed using the PIC server (http://pic.mbu.iisc.ernet.in/index.html).

Enzyme activity and protein assays

The substrate, *p*-nitrophenyl ferulate (*p*NPF), was synthesized according to a single-step method as reported previously (Hegde et al. 2009). Feruloyl esterase activity was determined by measuring the amount of *p*-nitrophenol (*p*NP) released from *p*NPF as described (Mastihuba et al. 2002), with minor modification. Briefly, the reaction mixture (eight volumes of 100 mM Na_2HPO_4–NaH_2PO_4 buffer (pH 5.5) containing 2.5 % (*V*/*V*) Triton X-100, one volume of 10 mM *p*NPF in dimethyl sulfoxide, and one volume of suitably diluted enzyme) was incubated at 45 °C for 10 min. The released *p*NP was measured at 410 nm using a spectrophotometer. One unit (U) of feruloyl esterase activity was defined as the amount of enzyme that released 1 μmol *p*NP per minute under the standard assay conditions as stated above.

The expressed protein was assayed by SDS-PAGE. The separated peptide bands were visualized by staining with Coomassie Brilliant Blue R-250 (Sigma, St. Louis, MO, USA), and molecular weights were estimated in comparison to the standard protein markers using Quantity One software. The protein content was measured with a BCA-200 Protein Assay Kit (Pierce, Rockford, IL, USA), using bovine serum albumin as the standard.

Construction of saturation mutagenesis library

After analysis of the B-factor and ΔΔG values of AnFaeA, two amino acid positions Ser33 and Asn92 in AuFaeA were selected for saturation mutagenesis. Based on the computer program CASTER (http://www.mpi-muelheim.mpg.de/reetz.html), five groups of degenerate codons for each position encoding 19 amino acids were designed for saturation mutagenesis (Table 1). Primers used for the creation of saturation mutagenesis libraries were listed in Table 2. Using the pPIC9K-*AufaeA* as template, the saturation mutagenesis of position Ser33 was firstly implemented according to the PCR technique as described previously (Sanchis et al. 2008). In the first stage of PCR, five groups of the mutagenic primer SM-33R (Table 2) separately annealed to the template with the antiprimer Fae-F and the amplified sequences were used as megaprimers in the second stage. Then, the template plasmids were digested using *Dpn*I, and the resulting five libraries were transformed into *E. coli* JM109, respectively. The five groups of *E. coli* transformants were separately accumulated and the plasmids were extracted to be linearized by *Sal*I. Finally, the five groups of linear mutated plasmids and pPIC9K-*AufaeA* were electroporated into *P. pastoris* GS115, respectively. Similarly, the saturation mutagenesis of position Asn92 was accomplished on the basis of a Ser33 variant with the best thermal stability.

Screening of the thermostable variants

According to Table 1, the corresponding colonies for 95 % coverage of the five groups of *P. pastoris* transformants were picked and induced by 1 % (*V*/*V*) methanol for 72 h to express the feruloyl esterases according to the instructions of Multi-Copy *Pichia* Expression Kit (Invitrogen, USA). After centrifugation at 8000 rpm for 10 min, the supernatant of each transformant was prepared for thermostability studies. For screening the thermostable variants, the supernatants of the transformants were incubated in the absence of substrate at 50 °C for 60 min, respectively. The ones with high residual activities (>50 %) were selected for further studies on thermal inactivation half-life ($t_{1/2}$) at 50 °C. The thermal inactivation half-life ($t_{1/2}$) was defined as the time when the residual activity of the recombinant feruloyl

Table 1 Analysis of codons for saturation mutagenesises of positions Ser33/Asn92

Degenerate codon[a]	Reverse complement codons[a]	No. of codons	No. of amino acids	No. of stops	Amino acids encoded	Colonies of 95 % coverage (1 position)[b]
GNS/BBG	SNC/CVV	8/9	5/8	0/0	ADEGV/ARGLPSWV	22/25
TDS/TDC	SHA/GHA	6/3	5/3	1/0	CLFWY/CFY	16/7
AHR/CAS	YDT/STG	6/2	4/2	0/0	IKMT/QH	16/4
CVT/AHR	ABG/YDT	3/6	3/4	0/0	RHP/IKMT	7/16
MAS/GAS	STK/STC	4/2	4/2	0/0	NQHK/DE	10/4

[a] N=A/C/G/T; B=C/G/T; D=A/G/T; S=G/C; H=A/C/T; R=A/G; V=A/C/G; M=A/C; Y=C/T; K=T/G

[b] Number of colonies to be screened for 95 % coverage (over-sampling) when two or three amino acid positions at a given site are randomized using a specific degenerate codon

Table 2 Sequences of the primers used for the creation of saturation mutagenesis libraries

Amino acid position	Primer sequence (5′-3′)[a]
Fae-F	GAATTCGCTTCCACGCAAGGCATCTC
SM-33R	CCTTTGATAATAGT$(XXX)_{33}$TGGAATATTG
SM-92R	TGTACCTCGCAATC$(XXX)_{92}$GCATTGAG

[a] The five reverse complement codons from Table 1 for saturation mutagenesises of positions Ser33/Asn92 in mutagenic primers SM-33R and SM-92R, respectively, are represented in X and enclosed with position 33 or 92 as the subscript

esterase, determined under the standard conditions, was 50 % of its original activity. Each of the *P. pastoris* transformant expressing thermostable feruloyl esterase was cultivated in YPD medium. The genomic DNA was extracted for feruloyl esterase gene PCR amplification with primers Fae-F and Fae-R (5′-GCGGCCGCTTACCAAGTACAAGCTCCG-3′). The PCR products were ligated into plasmid pUCm-T for sequence analysis to confirm the nucleotide changes. The Ser33 variant with the longest half-life ($t_{1/2}$) at 50 °C was defined to be the best one for the mutagenesis of position Asn92.

Purification of expressed feruloyl esterase

The expressed feruloyl esterase in the supernatant was salted out by adding ammonium sulfate $(NH_4)_2SO_4$ to 75 % saturation. The collected precipitate was dissolved and dialyzed in Na_2HPO_4–NaH_2PO_4 buffer (20 mM, pH 5.5). The dialyzed solution was concentrated by ultrafiltration using a 10-kDa cutoff membrane (Millipore, Billerica, MA, USA) and was loaded on a Sephadex G-50 column (Amersham Pharmacia Biotech, Uppsala, Sweden; 1.6 × 80 cm), followed by elution with the same buffer at a flow rate of 0.4 ml/min. Aliquots of 2 ml eluent containing recombinant feruloyl esterase were pooled and concentrated for further studies.

Enzymatic properties

Purified feruloyl esterases were functioned in the standard enzyme activity assay conditions except the changed temperatures to measure the temperature optima, and were incubated in the absence of substrate at 55 °C for different time to estimate their thermostability. The T_m values of proteins were measured using differential scanning (DSC) calorimeter (TA Instruments, New Castle, USA) at a temperature scanning range from 30 to 70 °C at a rate of 1 °C/min with nitrogen as carrier gas. The sample with concentration of 1.0 mg/ml was prepared after filtering through 0.22-μm millipore filters.

The pH optimum and stability, as well as metal ion and EDTA tolerance of the purified feruloyl esterases, were measured according to the methods as reported previously (Gong et al. 2013). The hydrolytic reaction rates (U/mg) of the purified feruloyl esterases were separately determined under the standard assay conditions, with a wide range of *p*NPF concentration (0.5 to 20.0 mM). Data were fitted to the Michaelis-Menten equation to generate K_m and k_{cat} values using a Graph-Pad Prism 5.0 software.

Results

Selection of candidate amino acids for mutagenesis

The amino acid sequence of feruloyl esterase (AuFaeA) from *A. usamii* was submitted into NCBI website for blast in Protein Data Bank database. Four crystal structures with PDB-IDs (1UWC, 2HL6, 1USW, and 2BJH) of AnFaeA from *A. niger* were searched out. After analysis of them, an ideal one 1UWC in a single-crystal structure with a resolution of 1.08 Å, which was highly homologous with AuFaeA in identity of 98 % for their primary structures, was finally selected for analyzing by B-FITTER software. Ten amino acids of

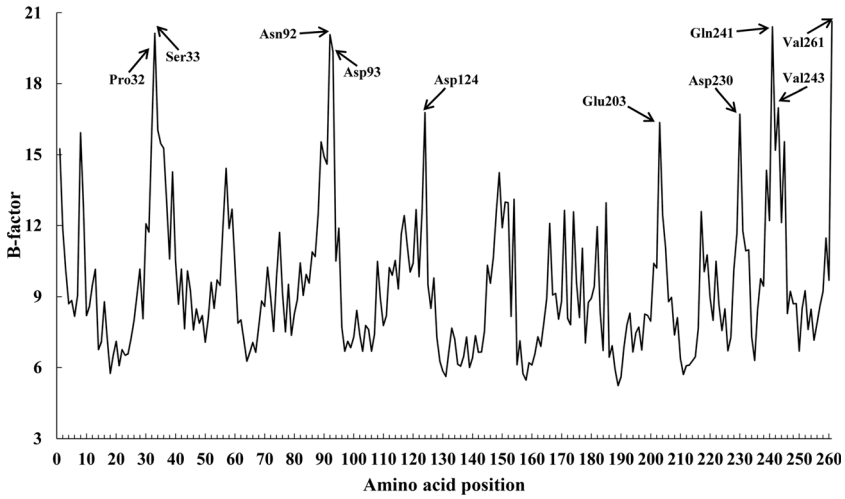

Fig. 1 The B-factors of amino acids of AnFaeA (1UWC). The 10 amino acids with the highest B-factor values are marked in a *bold arrow*

Table 3 The 10 amino acids of AnFaeA (1UWC) with the highest B-factor values

Residue	Residue seq. no.	B-factor value	Rank
Val	261	20.63	1
Gln	241	20.4	2
Ser	33	20.13	3
Asn	92	20.07	4
Asp	93	19.35	5
Val	243	16.98	6
Asp	124	16.78	7
Asp	230	16.71	8
Glu	203	16.36	9
Pro	32	16.08	10

AnFaeA with the highest B-factor values were generated and ranked (Fig. 1 and Table 3). The Val261 and Gln241 with B-factor values ranked 1 and 2 were rejected as following reasons: Gln241 was located near the catalytic triad within a distance of 6 Å, which could influence the enzymatic activity, and Val261 was located at the C-terminus of AnFaeA but lacked in AuFaeA. Two amino acids Ser33 and Asn92 with B-factor values ranked 3 and 4 were primarily selected as candidate sites for mutagenesis. Then, the ΔΔG values of AnFaeA caused by single-site saturation mutagenesis in positions Ser33 and Asn92 were calculated by PoPMuSiC. A protein is predicted to be stable when its ΔΔG values caused by mutation are less than 0 kcal/mol (Dehouck et al. 2011). The sum of negative ΔΔG values of positions Ser33 and Asn92 were −0.24 and −5.61 kcal/mol, which indicated these two positions could be mutated for stabilizing protein. Ultimately, based on the prediction of B-factor and ΔΔG values, the amino acid positions Ser33 and Asn92 in AuFaeA were determined for ISM.

Screening for thermostability enhanced variants

After the supernatants of S33 transformants were incubated in the absence of substrate at 50 °C for 60 min, six variants S33-1 to S33-6 were firstly screened out. The residual activities of them were more than 50 % of their original activities, while that of the wild type was lower than 50 % (Fig. 2a). Among them, the residual activity of S33-6 was more than 80 %. After sequence analysis, the changed amino acids at position Ser33

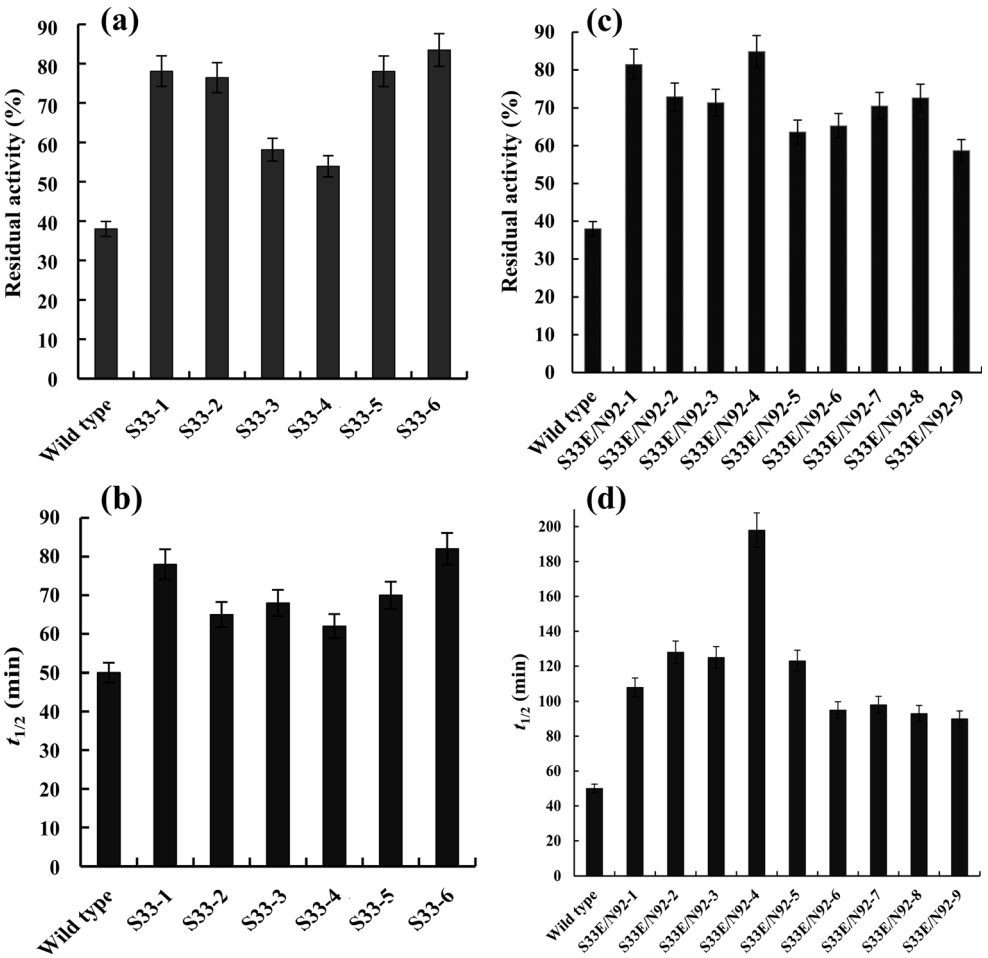

Fig. 2 Results of the screen. **a** The S33 variants were selected out with high residual activities (>50 %) after incubated in the absence of substrate at 50 °C for 60 min. **b** The thermal inactivation half-lives ($t_{1/2}$) of S33 variants screened at 50 °C. **c** The S33E/N92 variants were selected out with high residual activities (>50 %) after incubated in the absence of substrate at 50 °C for 60 min. **d** The half-lives ($t_{1/2}$) of S33E/N92 variants screened at 50 °C

in the six variants were Pro, Val, Ala, Arg, Asp, and Glu, respectively. The corresponding names of the six variants were S33P, S33V, S33A, S33R, S33D, and S33E. The thermal inactivation half-lives ($t_{1/2}$) of these six variants at 50 °C were 78, 65, 68, 62, 70, and 82 min, which were separately 28, 15, 18, 12, 20, and 32 min longer than that (50 min) of the wild type (Fig. 2b). Thus, the variant S33-6 (S33E) with the best thermostability was selected and its feruloyl esterase gene was used as template for the saturation mutagenesis of position Asn92. The screening process for thermostable S33E/N92 variants was similar to that for S33 variants. Compared to the residual activity of wild type at 50 °C for 60 min, nine variants S33E/N92-1 to S33E/N92-9 were screened out with their residual activities of higher than 50 % (Fig. 2c). Among them, the residual activities of S33E/N92-1, -2, -3, -4, -7, and -8 were more than 70 %. After sequence analysis, the changed amino acids at position Asn92 in the nine variants were Phe, Leu, Pro, Arg, Thr, Lys, Val, Ala, and Gly, respectively. The corresponding names of the nine variants were S33E/N92F, S33E/N92L, S33E/N92P, S33E/N92R, S33E/N92T, S33E/N92K, S33E/N92V, S33E/N92A, and S33E/N92G. Their half-lives ($t_{1/2}$) at 50 °C were 108, 128, 125, 198, 123, 95, 98, 93, and 90 min, which were separately 2.16-, 2.56-, 2.5-, 3.96-, 2.46-, 1.9-, 1.96-, 1.86-, and 1.8-folds longer than that of wild type, while 1.32-, 1.56-, 1.52-, 2.41-, 1.5-, 1.16-, 1.2-, 1.13-, and 1.1-folds longer than that of variant S33-6 (S33E) (Fig. 2d). In general, the variant S33E/N92-4 (S33E/N92R) was the most thermostable one owing to ISM method.

Properties of S33-6 (S33E) and S33E/N92-4 (S33E/N92R)

The purified variants S33-6 (S33E) and S33E/N92-4 (S33E/N92R) showed the similar apparent molecular weights (about 36.0 kDa) to the wild type. The temperature optima of S33-6 (S33E) and S33E/N92-4 (S33E/N92R) were 49 and 51 °C, which were separately 4 and 6 °C higher than that (45 °C) of the wild type (Fig. 3). The half-lives ($t_{1/2}$) of S33-6 (S33E) and S33E/N92-4 (S33E/N92R) at 55 °C were 18 and 35 min, which were 1.2- and 2.33-folds longer than that (15 min) of wild type, respectively (Fig. 4). Their T_m values were 41.7 and 44.5 °C, which were slightly higher than that (39.8 °C) of the wild type (Fig. 5). Both of the pH optima of S33-6 (S33E) and S33E/N92-4 (S33E/N92R) were 5.5. The S33-6 (S33E) was stable at a pH range of 4.0–8.0 with a residual activity of more than 50 %, whereas the range for S33E/N92-4 (S33E/N92R) was 4.0–7.5. They were not greatly affected by tested ions and EDTA (data not shown). These properties were not significantly different from those of wild type. The catalytic efficiencies (k_{cat}/K_m) of S33-6 (S33E) and S33E/N92-4 (S33E/N92R) tested at 45 °C were 2435 and

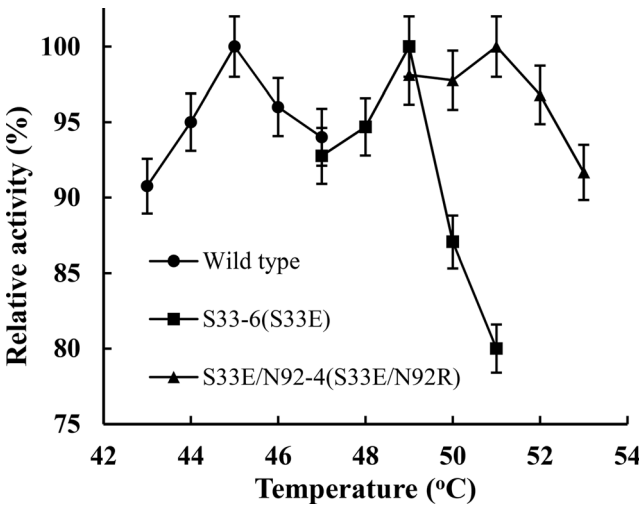

Fig. 3 The temperature optima of variants S33-6 (S33E), S33E/N92-4 (S33E/N92R), and the wild type

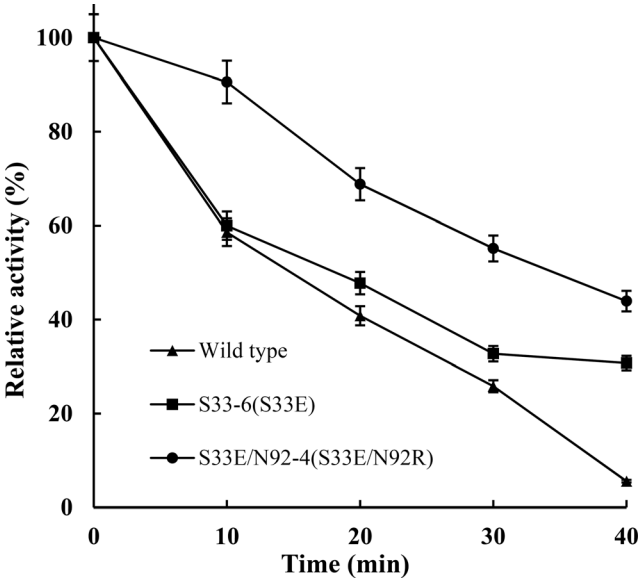

Fig. 4 The half-lives ($t_{1/2}$) of variants S33-6 (S33E), S33E/N92-4 (S33E/N92R), and the wild type at 55 °C

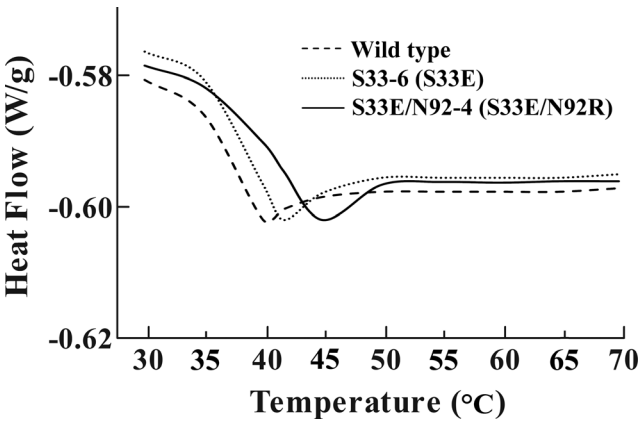

Fig. 5 The melting curves of variants S33-6 (S33E), S33E/N92-4 (S33E/N92R), and the wild type. The scanning temperature range is from 30 to 70 °C at a scan rate of 1 °C/min

Table 4 The ΔΔG values of S33 and S33E/N92 variants

Variant	ΔΔG (kcal/mol)									The sum of negative ΔΔG[a]
	−1	−2	−3	−4	−5	−6	−7	−8	−9	
S33	−0.19	0.28	−0.05	0.55	0.25	0.33	–	–	–	−0.24
S33E/N92	−0.02	−0.12	−0.79	−0.39	−0.4	−0.34	−0.58	−0.83	0.12	−5.61

[a] The sum of all the negative ΔΔG of S33 or S33E/N92 variants, which were screened out and those not be, predicted by PoPMuSiC

2466 mM^{-1} min^{-1}, which were slightly higher than that (2235 mM^{-1} min^{-1}) of wild type, indicating that the mutant enzymes were expected to show higher activities at elevated temperature.

Discussion

An advantage of the *P. pastoris* expression system is the high purity of the expressed recombinant protein, as described in the Multi-Copy *Pichia* Expression Kit (Invitrogen, USA). Purities of recombinant *A. usamii* xylanase and *Aspergillus sulphureus* β-mannanase expressed in *P. pastoris* GS115 and X-33 have been reported to be as high as 90 and 97 %, respectively (Yin et al. 2013). *P. pastoris* was becoming a popular host expressing heterologous proteins and started being applied in directed evolution recently (Fernández et al. 2010). Although multiple insertion events could occur spontaneously at about 1–10 % of the single insertion events, the screening process, which involves the measurement of residual activities, would not be affected (Zhang et al. 2012).

The degenerate codon NNK (N: A/C/G/T; K: G/T) containing 32 codons and encoding all the 20 amino acids was commonly applied to saturation mutagenesis (Tian et al. 2013). Based on the computer program CASTER, the number of colonies that should be screened for 95 % coverage in the case of randomization at one amino acid position was 94. Here, five groups of degenerate codons encoding 19 amino acids were designed, respectively, for saturation mutagenesises of positions Ser33 and Asn92 in AuFaeA. The corresponding colonies should be screened according to CASTER were only 71 and 56, which made the amount of *P. pastoris* transformants to be screened significantly reduced. Instead of applying the conventional PCR methods for construction of saturation mutagenesis libraries (Zheng et al. 2004), an improved PCR method was used for its high applicability and rapidity in performing saturation mutagenesis. Although the QuikChange™ and other methods for generating a site saturation mutagenesis library were developed rapidly very recently (Jain and Varadarajan 2014; Taniguchi et al. 2013), the method we used avoids traditional subcloning steps and requires only one randomized oligonucleotide per library plus an antiprimer (non-mutagenic oligonucleotide). The antiprimer can be designed in an area that avoids palindromes, hairpins, or overlapping regions with the mutagenic primer and can be used repeatedly in different saturation mutagenesis reactions (Sanchis et al. 2008). The PCR technique guaranteed the quality of mutagenesis libraries and to some extent made the screening effort simplified.

The PoPMuSiC algorithm is a tool for the computer-aided design of mutant proteins with controlled stability properties. It evaluates the changes in stability of a given protein or peptide under single-site mutations, on the basis of the protein's structure. The PoPMuSiC algorithm has been successfully applied to improve the thermostability of other proteins. For example, two variants Josephin R103G and S81A showed an increase in stability with a shift in the midpoint of the transition from 51.3 to 55.9 and 54.1 °C, respectively (Saunders

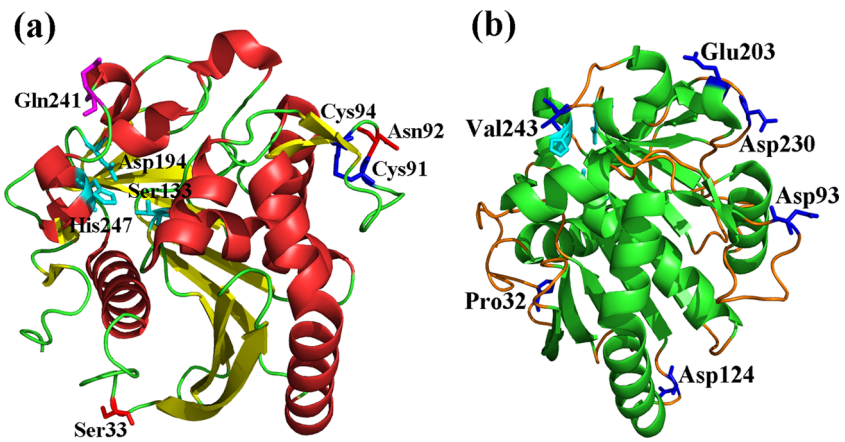

Fig. 6 The 3D structures of AuFaeA and AnFaeA. **a** The amino acids Gln241, Ser33, Asn92, disulfide bridge (Cys91-Cys94), and the catalytic triad Ser133-Asp194-His247 in AuFaeA are shown in stick. **b** The Asp93, Val243, Asp124, Asp230, Glu203, and Pro32 in AnFaeA with high B-factors ranked 5 to 10 are shown in *stick*

et al. 2011). The thermostabilities of two single mutations D93G and S18F of a feruloyl esterase A from *A. niger* were improved with an increased half-life from 8 min (wild type) to 9.4 and 60.5 min at 50 °C, respectively (Zhang and Wu 2011). These changes in stability were in agreement with the PoPMuSiC predictions. Interestingly in this work, the S33-1 (S33P) and S33E/N92-8 (S33E/N92A) predicted as the most favorable (the lowest ΔΔG) by PoPMuSiC were not the best variants (Table 4). Nevertheless, the sum of negative ΔΔG values of amino acid positions, to some extent, could still indicate the mutation for stabilizing protein.

The thermostability of protein could be increased by subtle changes in sequence and structure (Taylor and Vaisman 2010). Some amino acids, such as Asn, Gln, Met, Cys, Ser, and Thr,

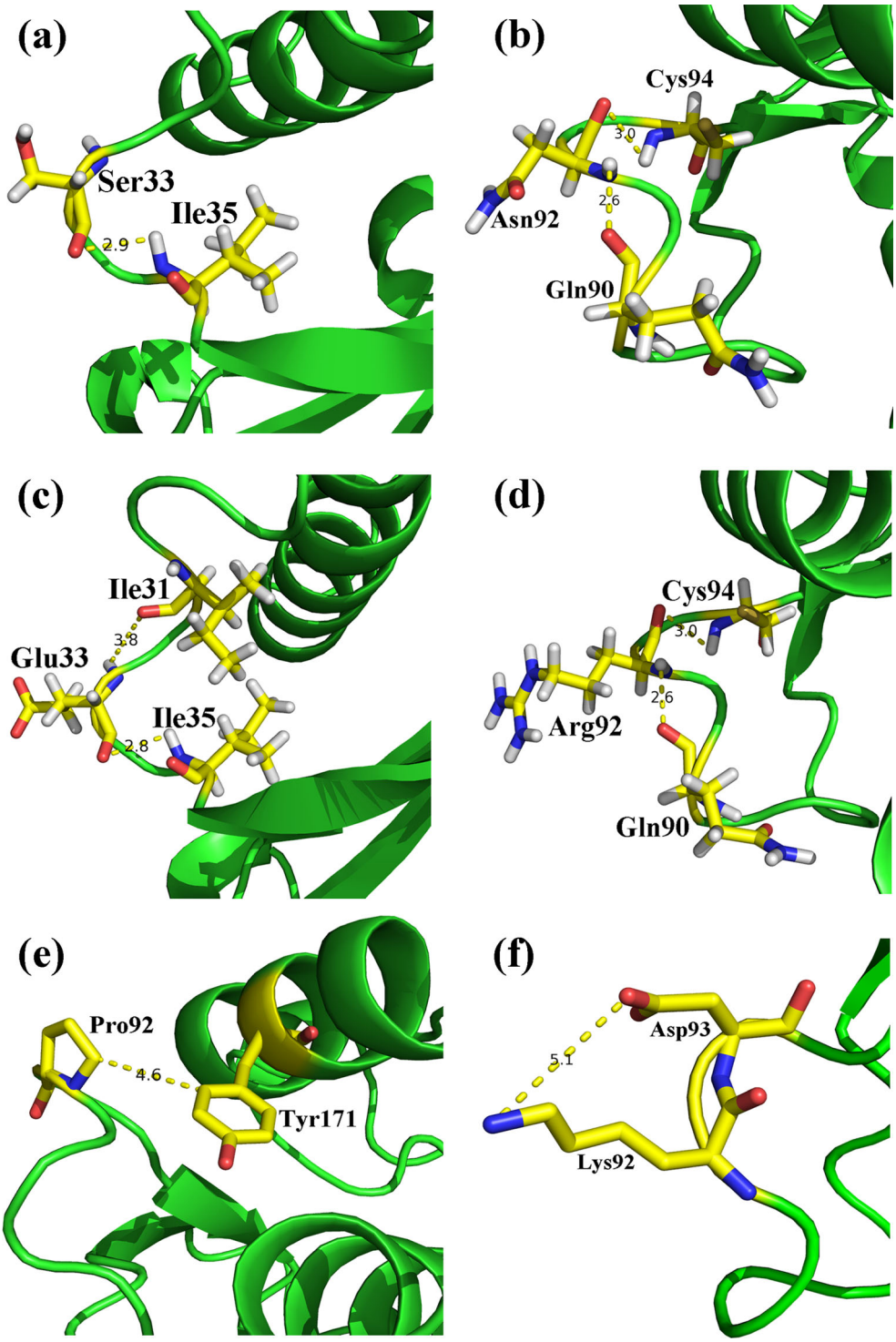

Fig. 7 The putative intramolecular interactions around positions 33 and/or 92 in AuFaeA and S33E/N92 variants. **a**, **b** The hydrogen bonds in main chain-main chain around position 33 and 92 in AuFaeA. **c**, **d** The hydrogen bonds in main chain–main chain around position 33 and 92 in S33E/N92-4 (S33E/N92R). **e** The hydrophobic interaction between Pro92 and Tyr171 within 5 Å in S33E/N92-3 (S33E/N92P). **f** The salt bridge between Lys92 and Asp93 within 6 Å in S33E/N92-6 (S33E/N92K)

are thermolabile because they tend to undergo deamidation (Asn and Gln) or oxidation (Met, Cys, Ser, and Thr) at high temperatures (Kumar et al. 2000). The Ser33 and Asn92 selected for mutagenesis were reasonable. However, it was strange that the thermostability of variant S33E/N92-5 (S33E/N92T) was improved by 2.46-fold than that of wild type. The amino acids Pro, Leu, Val, Arg, Lys, Asp, and Glu are relatively thermostable (Pack and Yoo 2004). Proline has the lowest conformational entropy since its rigid pyrrolidine ring constrains the main chain dihedral angel φ to −63 ± 15° and leads to the decrease of conformational freedom of Cα–N rotation. Besides, proline also restricts the conformation of residue preceding it in a polypeptide chain (Yu and Huang 2014). Introduction of proline residues at certain positions has been used successfully to improve the thermostabilities of many enzymes (Tian et al. 2010; Wang et al. 2014). Compared to proline, glycine, the only amino acid lacking a β-carbon, has the highest conformational entropy. Thus, the variant S33E/N92-9 (S33E/N92G) might be explained by other reasons for its enhanced thermostability. Leucine and valine have a large hydrophobic alkyl side chain, which could increase the protein hydrophobicity and further increase the stability. Arginine, lysine, aspartic acid, and glutamic acid are charged amino acids, which could easily arouse the formation of hydrogen bonds and salt bridges, and then contribute to thermostability (Bai et al. 2014; Jun et al. 2014). The majority of variants with higher thermostability in this work could be elucidated by the above reasons, except the S33-3 (S33A), S33E/N92-1 (S33E/N92F), and S33E/N92-8 (S33E/N92A), which probably be expounded by some other increased intramolecular interactions due to the mutational amino acids.

The amino acid located at loop structure of protein was important for thermostability. The Ser33 and Asn92 were located at two long loops (Fig. 6a), which were separately composed of about 10 amino acids. The length, rigidity or amino acid composition of a loop could relate to the protein thermostability (Balasco et al. 2013), since it is commonly unstable and easily broken. The mutational amino acids here at the loops could strengthen the rigidity of two loops with adjacent amino acids, and further improve the thermostability of AuFaeA. So far, it was easier to understand the reason for thermostable variant S33E/N92-9 (S33E/N92G). The Asn92 is located between two cysteines (Cys91 and Cys94), which form a disulfide bridge (Fig. 6a). Although the glycine has the highest conformational entropy, the interaction between these two cysteines could still be strengthened for the smallest mutational amino acid Gly. The Asp93, Val243, Asp124, Asp230, Glu203, and Pro32 in AnFaeA with high B-factors ranked 5 to 10 were predicted to be flexible (Table 3), which probably be deduced by that they were all located at loops (Fig. 6b). Thus, these amino acid positions in AuFaeA were expected to be modified for thermostability improvement.

In addition, the intramolecular interactions in AuFaeA and its S33E/N92 variants were separately analyzed using the PIC server. Except S33E/N92-3 (S33E/N92P) and S33E/N92-6 (S33E/N92K), all the other variants (S33E/N92-4 (S33E/N92R) was as an example shown in Fig. 7) had four putative hydrogen bonds in main chain–main chain around positions 33 and 92, while one around position 33 was lacked in AuFaeA. In S33E/N92-3 (S33E/N92P), a new putative hydrophobic interaction between Pro92 and Tyr171 could be formed within 5 Å (Fig. 7e). In S33E/N92-6 (S33E/N92K), a new putative salt bridge between Lys92 and Asp93 could be formed within 6 Å (Fig. 7f). These intramolecular interactions in the variants would play important roles in their thermostabilities. Reportedly, several variants of a *Bacillus circulans* xylanase with strengthened hydrophobic interactions in local structure were much more thermostable than the wild type (Kim et al. 2012). A *E. coli* AppA phytase was significantly improved in thermostability by introducing several salt bridges (Fei et al. 2013). In conclusion, the thermostability of AuFaeA was obviously enhanced by ISM based on computer-aided design. It indicates that the combination of rational design and directed evolution is also considerable for protein engineering.

Acknowledgments The authors are grateful to Prof. Xianzhang Wu (School of Biotechnology, Jiangnan University, Jiangsu, China) for providing technical assistance.

Funding This work was financially supported by the Fundamental Research Fund for the Central Universities of China (No. JUDCF13011, JUSRP51412B), the Postgraduate Innovation Training Project of Jiangsu (No. CXZZ13_0757), and the National Training Programs of Innovation and Entrepreneurship for Undergraduates (201410295037).

Conflict of interest The authors declare that they have no competing interests.

Ethical statement This article does not contain any studies with human participants or animals performed by any of the authors.

References

Abokitse K, Wu M, Bergeron H, Grosse S, Lau PCK (2010) Thermostable feruloyl esterase for the bioproduction of ferulic acid from triticale bran. Appl Microbiol Biotechnol 87:195–203

Badieyan S, Bevan DR, Zhang C (2012) Study and design of stability in GH5 cellulases. Biotechnol Bioeng 109:31–44

Bai W, Zhou C, Xue Y, Huang CH, Guo RT, Ma Y (2014) Three-dimensional structure of an alkaline xylanase Xyn11A-LC from alkalophilic *Bacillus* sp. SN5 and improvement of its thermal performance by introducing arginines substitutions. Biotechnol Lett 36: 1495–1501

Balasco N, Esposito L, Simone AD, Vitagliano L (2013) Role of loops connecting secondary structure elements in the stabilization of proteins isolated from thermophilic organisms. Protein Sci 22:1016–1023

Chen CC, Luo HL, Han X, Lv P, Ko TP, Peng W, Huang CH, Wang K, Gao J, Zheng Y, Yang Y, Zhang J, Yao B, Guo RT (2014) Structural perspectives of an engineered β-1,4-xylanase with enhanced thermostability. J Biotechnol 189:175–182

Crepin VF, Faulds CB, Connerton IF (2004) Functional classification of the microbial esterases. Appl Microbiol Biotechnol 63:647–652

Dehouck Y, Kwasigroch JM, Gilis D, Rooman M (2011) PoPMuSiC 2.1: a web server for the estimation of protein stability changes upon mutation and sequence optimality. BMC Bioinformatics 12:151

Faulds CB (2010) What can feruloyl esterases do for us? Phytochem Rev. 9:121–132

Fei B, Xu H, Cao Y, Ma S, Guo H, Song T, Qiao D, Cao Y (2013) A multi-factors rational design strategy for enhancing the thermostability of *Escherichia coli* AppA phytase. J Ind Microbiol Biotechnol 40:457–464

Fernández L, Jiao N, Soni P, Gumulya Y, de Oliveira LG, Reetz MT (2010) An efficient method for mutant library creation in *Pichia pastoris* useful in directed evolution. Biocatal Biotransfor 28:122–129

Gong YY, Yin X, Zhang HM, Wu MC, Tang CD, Wang JQ, Pang QF (2013) Cloning, expression of a feruloyl esterase from *Aspergillus usamii* E001 and its applicability in generating ferulic acid from wheat bran. J Ind Microbiol Biotechnol 40:1433–1441

Hegde S, Srinivas P, Muralikrishna G (2009) Singe-step synthesis of 4-nitrophenyl ferulate for spectrophotometric assay of feruloyl esterases. Anal Biochem 387:128–129

Hermoso JA, Sanz-Aparicio J, Molina R, Juge N, González R, Faulds CB (2004) The crystal structure of feruloyl esterase A from *Aspergillus niger* suggests evolutive functional convergence in feruloyl esterase family. J Mol Biol 338:495–506

Jain PC, Varadarajan R (2014) A rapid, efficient, and economical inverse polymerase chain reaction-based method for generating a site saturation mutant library. Anal Biochem 449:90–98

Jun C, Joo JC, Lee JH, Kim YH (2014) Thermostabilization of glutamate decarboxylase B from *Escherichia coli* by structure-guided design of its pH-responsive N-terminal interdomain. J Biotechnol 174:22–28

Kim T, Joo JC, Yoo YJ (2012) Hydrophobic interaction network analysis for thermostabilization of a mesophilic xylanase. J Biotechnol 161: 49–59

Kumar S, Tsai CJ, Nussinov R (2000) Factors enhancing protein thermostability. Protein Eng 13:179–191

Li Y, Cirino PC (2014) Recent advances in engineering proteins for biocatalysis. Biotechnol Bioeng 111:1273–1287

Mastihuba V, Kremnický L, Mastihubová M, Willett JL, Côté GL (2002) A spectrophotometric assay for feruloyl esterases. Anal Biochem 309:96–101

Pack SP, Yoo YJ (2004) Protein thermostability: structure-based difference of amino acid between thermophilic and mesophilic proteins. J Biotechnol 111:269–277

Rakotoarivonina H, Hermant B, Chabbert B, Touzel JP, Remond C (2011) A thermostable feruloyl-esterase from the hemicellulolytic bacterium *Thermobacillus xylanilyticus* releases phenolic acids from non-pretreated plant cell walls. Appl Microbiol Biotechnol 90:541–552

Reetz MT, Carballeira JD, Vogel A (2006) Iterative saturation mutagenesis on the basis of B factors as a strategy for increasing protein thermostability. Angew Chem Int Edit 45:7745–7751

Reetz MT, Soni P, Fernández L, Gumulya Y, Carballeira JD (2010) Increasing the stability of an enzyme toward hostile organic solvents by directed evolution based on iterative saturation mutagenesis using the B-FIT method. Chem Commun 46:8657–8658

Sanchis J, Fernández L, Carballeira JD, Drone J, Gumulya Y, Höbenreich H, Kahakeaw D, Kille S, Lohmer R, Peyralans JJ, Podtetenieff J, Prasad S, Soni P, Taglieber A, Wu S, Zilly FE, Reetz MT (2008) Improved PCR method for the creation of saturation mutagenesis libraries in directed evolution: application to difficult-to-amplify templates. Appl Microbiol Biotechnol 81:387–397

Saunders HM, Gilis D, Rooman M, Dehouck Y, Robertson AL, Bottomley SP (2011) Flanking domain stability modulates the aggregation kinetics of a polyglutamine disease protein. Protein Sci 20: 1675–1681

Shallom D, Shoham Y (2003) Microbial hemicellulases. Curr Opin Microbiol 6:219–228

Silva IR, Larsen DM, Jers C, Derkx P, Meyer AS, Mikkelsen JD (2013) Enhancing RGI lyase thermostability by targeted single point mutations. Appl Microbiol Biotechnol 97:9727–9735

Stephens DE, Khan FI, Singh P, Bisetty K, Singh S, Permaul K (2014) Creation of thermostable and alkaline stable xylanase variants by DNA shuffling. J Biotechnol 187:139–146

Taniguchi N, Nakayama S, Kawakami T, Murakami H (2013) Patch cloning method for multiple site-directed and saturation mutagenesis. BMC Biotechnol 13:91

Taylor TJ, Vaisman II (2010) Discrimination of thermophilic and mesophilic proteins. BMC Struct Biol 10(Suppl 1):S5

Tian J, Wang P, Gao S, Chu X, Wu N, Fan Y (2010) Enhanced thermostability of methyl parathion hydrolase from *Ochrobactrum* sp. M231 by rational engineering of a glycine to proline mutation. FEBS J 277:4901–4908

Tian J, Wang P, Huang L, Chu X, Wu N, Fan Y (2013) Improving the thermostability of methyl parathion hydrolase from *Ochrobactrum* sp. M231 using a computationally aided method. Appl Microbiol Biotechnol 97:2997–3006

Turner P, Mamo G, Karlsson EN (2007) Potential and utilization of thermophiles and thermostable enzymes in biorefining. Microb Cell Fact 6:9–31

Wang K, Luo H, Tian J, Turunen O, Huang H, Shi P, Hua H, Wang C, Wang S, Yao B (2014) Thermostability improvement of a *Streptomyces* xylanase by introducing proline and glutamic acid residues. Appl Microbiol Biotechnol 80:2158–2165

Yin X, Li JF, Wang JQ, Tang CD, Wu MC (2013) Enhanced thermostability of a mesophilic xylanase by N-terminal replacement designed by molecular dynamics simulation. J Sci Food Agric 93:3016–3023

Yu H, Huang H (2014) Engineering proteins for thermostability through rigidifying flexible sites. Biotechnol Adv 32:308–315

Zhang HM, Li JF, Wang JQ, Yang YJ, Wu MC (2014) Determinants for the improved thermostability of a mesophilic family 11 xylanase predicted by computational methods. Biotechnol Biofuels 7:3

Zhang SB, Pei XQ, Wu ZL (2012) Multiple amino acid substitutions significantly improve the thermostability of feruloyl esterase A from *Aspergillus niger*. Bioresource Technol 117:140–147

Zhang SB, Wu ZL (2011) Identification of amino acid residues responsible for increased thermostability of feruloyl eaterase A from *Aspergillus niger* using the PoPMuSiC algorithm. Bioresource Technol 102:2093–2096

Zhang SB, Zhai HC, Wang L, Yu GH (2013) Expression, purification and characterization of a feruloyl esterase A from *Aspergillus flavus*. Protein Expres Purif 92:36–40

Zheng H, Liu Y, Sun M, Han Y, Wang J, Sun J, Lu F (2014) Improvement of alkali stability and thermostability of *Paenibacillus campinasensis* family-11 xylanase by directed evolution and site-directed mutagenesis. J Ind Microbiol Biotechnol 41:153–162

Zheng L, Baumann U, Reymond JL (2004) An efficient one-step site-directed and site-saturation mutagenesis protocol. Nucleic Acids Res 32:e115